ELSEVIER

Physica B 221 (1996) 370–376

PHYSICA B

Neutron diffraction and reflectivity studies of the Cr Néel transition in Fe/Cr (0 0 1) superlattices[1]

Eric E. Fullerton[a,*], S. Adenwalla[a], G.P. Felcher[a], K.T. Riggs[a,2], C.H. Sowers[a], S.D. Bader[a], J.L. Robertson[b]

[a]*Materials Science Division, Argonne National Laboratory, Argonne, IL 60439, USA*
[b]*Solid State Division, Oak Ridge National Laboratory, Oak Ridge, TN, USA*

Abstract

The effects on the interlayer coupling of the Cr Néel transition is studied in Fe/Cr(0 0 1) superlattices. The Néel transition is suppressed for Cr layer thickness < 42 Å. For > 42 Å of Cr, the Néel temperature T_N initially increases rapidly and then asymptotically approaches its bulk value with a three-dimensional transition-temperature shift exponent value of $\lambda = 1.4 \pm 0.3$. Neutron diffraction confirms both the Cr antiferromagnetic order and the existence of the incommensurate, transverse spin density wave whose nesting wave vector is the same as that of bulk Cr. The ordering of the Cr dramatically alters the coupling of the Fe layers. The biquadratic Fe interlayer coupling observed for $T > T_N$ vanishes below T_N as confirmed by polarized neutron reflectivity. The behavior can be understood in terms of finite-size and spin frustration effects at rough Fe–Cr interfaces.

1. Introduction

New and interesting thin-film magnetic phenomena have been observed in Fe/Cr(0 0 1) trilayers and superlattices, including oscillatory interlayer coupling [1–4], giant magnetoresistance [5] and biquadratic interlayer coupling [6]. The question is how much of the richness of the system relates to the magnetic properties of Cr? Bulk Cr is an intinerant antiferromagnet (AF) which forms an incommensurate spin density wave (SDW) below the Néel temperature $T_N = 311$ K [7]. The SDW is characterized by a wave vector $\boldsymbol{Q}$ determined by the nested feature of the $\langle 1\,0\,0 \rangle$ direction of the Cr Fermi surface. In Fe/Cr/Fe(0 0 1) structures, two oscillatory periods have been observed: a short, 2.1-monolayer (ML) period [3] which is directly related to $\boldsymbol{Q}$, and a long, 18 Å period which is independent of crystallographic orientation [8]. Short-period oscillations are only observed in samples with atomically smooth Cr interfaces. Atomic steps average out the short-period coupling leaving only the long-period oscillations [9].

Theoretical models of the oscillatory coupling utilize band-structure modified Ruderman–Kittel–Kasuya–Yosida (RKKY) treatments of the spacer [10] as well as spin-dependent quantum-well treatments [11]. In these approaches, the coupling periods are governed by spanning vectors that join extremal points of the Fermi surface normal to the layering direction. The interlayer coupling is described by a coupling energy term of the

* Corresponding author.

[1] Work at ANL supported by the US Department of Energy, Basic Energy Sciences – Materials Sciences, under contract No. W-31-109-ENG-38. Work at ORNL supported by the US Department of Energy, Division of Materials Sciences, under contract No. DE-AC05-84OR21400.

[2] Permanent address: Department of Physics, Stetson University, DeLand, FL 32720, USA.

0921-4526/96/$15.00
SSDI 0921-4526(95)00951-5

form $J_1 \boldsymbol{m}_1 \cdot \boldsymbol{m}_2$, where J_1 is the bilinear coupling constant and $\boldsymbol{m}_1$, $\boldsymbol{m}_2$ are the magnetization of two adjacent ferromagnetic layers. In addition to the antiferromagnetic (AF) and ferromagenetic (F) alignments predicted by the Heisenberg expression, it was discovered in Fe/Cr(0 0 1) trilayers that 90° alignment [6] of adjacent layers occurred in transition regions between AF and FM coupling, where the bilinear coupling constant J_1 is small. To describe this coupling, an additional phenomenological term was included in the coupling energy of the form $J_2(\boldsymbol{m}_1 \cdot \boldsymbol{m}_2)^2$ where J_2 is a biquadratic coupling constant. Biquadratic coupling and/or the presence of a J_2 term in the coupling energetics has been observed in a number of systems [12–17].

The origin of the biquadratic coupling is less well understood than the bilinear coupling and has been attributed either to intrinsic properties of the spacer layer or to extrinsic mechanisms. Intrinsic biquadratic coupling arises from series expansions of the exchange energy of the form $\sum J_n(\boldsymbol{m}_1 \cdot \boldsymbol{m}_2)^n$ where J_2 arises from the $n = 2$ term [18]. However, the magnitude of J_2 estimated in such treatments are, in general, much smaller than experimentally observed values. As a result, a number of extrinsic mechanisms which, in general, depend on the structure of the samples (e.g. dipolar fields resulting from rough interfaces [19]) have been proposed. Slonczewski proposed two mechanisms for biquadratic coupling: fluctuations in the spacer thickness which averages over a short-period oscillation [20,21], and superparamagnetic impurities within the spacer ("loose spins") [21]. The first mechanism is particularly relevant in Fe/Cr(0 0 1) because of the prominent short-period coupling observed in this system. The mechanism assumes that the Cr layer can be described by terraces separated by monoatomic steps. The coupling across each terrace region will be F or AF and will alternate from one neighboring terrace to the next. If the terrace widths are small compared to the characteristic size of an Fe domain, the energy of the system is lowered by perpendicular alignment of the entire Fe layer magnetization with respect to that of the adjacent Fe layer. The fluctuation model recently was extended to include the intrinsic AF ordering of Cr or Mn spacers, and is referred to as a proximity magnetism model. The form of the energy expression is

$$E(\Delta\theta) = \frac{J_2}{\pi^2}[(\Delta\theta)^2 + (\Delta\theta - \pi)^2], \tag{1}$$

where $\Delta\theta$ is the relative angle between adjacent magnetic layers [22]. Although, these models can explain a number of experimental observations, the nature of the magnetic ordering of the Cr in the presence of a stepped or rough interface and its role on the interlayer coupling are not known.

Recent experiments on Fe/Cr(0 0 1) superlattices determined T_N values for relatively thick (> 42 Å) Cr spacers [23]. Also the magnetic properties of the superlattices were dramatically altered at T_N. For $T > T_N$, the magnetic properties were consistent with 90° coupling of adjacent Fe layers, while for $T < T_N$ the layers appeared uncoupled. In this paper neutron scattering is used to complement these previous results. The paper is divided into four sections: (i) experimental procedures, (ii) transport and neutron diffraction results that determine the Cr layer thickness dependence of T_N, (iii) magnetization, magnetotransport and polarized neutron reflectivity characterizations of the interlayer magnetic coupling of the Fe layers, and (iv) discussions and conclusions.

2. Experimental procedures

Epitaxial (0 0 1)-[Fe(14 Å)/Cr]$_N$ superlattices were grown by DC magnetron sputtering onto MgO(0 0 1) single-crystal substrates. A 100 Å Cr(0 0 1) base layer was deposited at 600°C onto the MgO prior to superlattice growth which occurred at 75–180°C. The Cr thickness was varied from 8 to 190 Å and N was adjusted for most experiments such that the superlattice thickness was ≈ 1000 Å. For the neutron diffraction measurements, N, however, was adjusted so the total Cr thickness was ≥ 1 μm. Separate samples were made on 2.5×2.5 cm^2 substrates for the neutron reflectivity and diffraction measurements. Magnetization, magnetoresistance, and neutron reflectivity measurements were made with the applied field H along both the Fe[1 0 0] easy axis and the [1 1 0] hard axis. The magnetization was measured between 10 and 350 K in a SQUID magnetometer. Transport properties were measured using a standard, four-terminal DC technique with a constant current source. The reflectivity was measured at the POSY1 beamline at the Intense Pulsed Neutron Source, Argonne National Laboratory. The neutron diffraction was measured at beamline HB-2 at the High-Flux Integral Reactor, Oak Ridge National Laboratory. The structure was characterized by X-ray diffraction.

Shown in Fig. 1 is a high-angle X-ray diffraction scan about the Cr(0 0 2) position for an [Fe(14 Å)/Cr(115 Å)]$_{100}$ sample. The Fe/Cr(0 0 2) peak with multiple satellite reflections confirms the (0 0 2)-growth orientation and the layering. The asymmetry in the diffraction peaks results from a small K_{α_2} contribution. Fitting the (0 0 2) peak position and relative satellite intensities yield Fe and Cr(0 0 2) spacings of 1.435 ± 0.010 and 1.445 ± 0.003 Å, respectively, indicating a small $\approx 0.2\%$ strain of the Cr layer. The crystal coherence length, estimated from the width of the Fe/Cr(0 0 2) peak via Scherrer's equations, is > 1500 Å. For the thinner samples (total

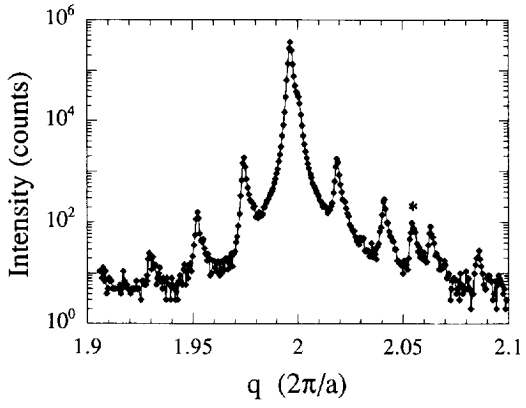

Fig. 1. High-angle X-ray diffraction spectrum from an [Fe(14 Å)/Cr(115 Å)]$_{100}$ superlattice about the Cr (002) position (a = 2.884 Å). The asymmetry of the main diffraction peak results from a small K_{α_2} contribution to the scattering. The asterisk marks a substrate peak.

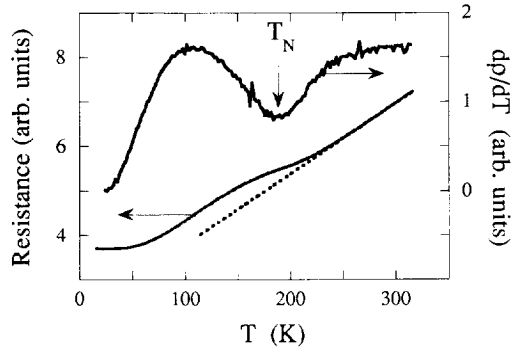

Fig. 2. Resistance measurements on the [Fe(14 Å)/Cr(74 Å)]$_{20}$ superlattice showing the Néel transition of the Cr. T_N is defined as the minimum in the dρ/dT curve.

thickness $\approx$1000 Å) the crystal coherence lengths are $\approx$400 Å [8]. Rocking curves through the (0 0 2) position gives mosaic spreads $< 1^\circ$ indicative of a high degree of crystal orientations. In-plane diffraction scans show the expected epitaxial relationship: Fe/Cr[100]//MgO[110].

3. Measurement of T_N

Transport measurements provide a standard technique to identify T_N in Cr and Cr alloys [7,24]. The resistivity ρ is enhanced above its paramagnetic value as T decreases through T_N. This increase in ρ is attributed to energy gaps opening on the nested parts of the Fermi surface [18]. Shown in Fig. 2 are ρ versus-T results for the [Fe(14 Å)/Cr(74 Å)]$_{20}$ superlattice used in the neutron reflectivity measurements. An anomaly in ρ is observed as an increase above its expected linear behavior shown by the dashed line. The transition is considerably broader than the singularity observed in single-crystal Cr. T_N is operationally defined as the point of inflection in the ρ versus T curve, as usual, and is 187 $\pm$ 5 K for the sample in Fig. 2.

Magnetic scattering of neutrons or X-rays from the AF SDW in Cr results in satellites at $(0, 0, 1 \pm \delta)$ positions [7], where the incommensurability δ is given by $1 - aQ/2\pi$ and a = 2.884 Å is the Cr lattice spacing. In bulk Cr, δ varies from 0.037 at T_N to 0.048 at 10 K, corresponding to SDW periods (a/δ) of 78 and 60 Å, respectively. Shown in Fig. 3 are neutron scans about the Cr(0 0 1) position (located at q = 1 in units of $2\pi/a$) for [Fe(14 Å)/Cr(115 Å)]$_{100}$ measured at different temperatures. The dashed lines indicate the expected $(1 + \delta)$ and

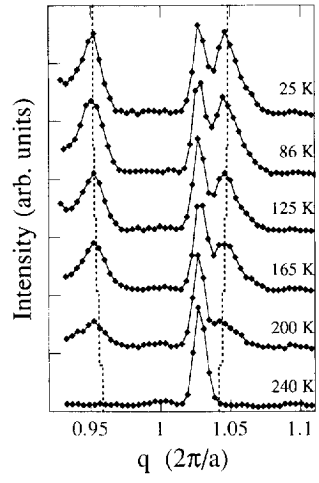

Fig. 3. Neutron diffraction results from an [Fe(14 Å)/Cr(115 Å)]$_{100}$ superlattice about the Cr (0 0 1) position. The dashed lines indicate the expected $(1 + \delta)$ and $(1 - \delta)$ satellites positions for bulk Cr. The T independent peak at q = 1.027 results from the substrate.

$(1 - \delta)$ satellites positions for bulk Cr. Satellites peaks are indeed observed near the expected bulk positions and decrease in intensity with increasing T. The strong T dependence confirms the magnetic origin of these peaks. The T-independent peak at q = 1.027 is the MgO(0 0 6) reflection from the $\lambda/4$ neutrons reflected from the Si(1 1 1) monochromator. An intense MgO(0 0 4) reflection from the $\lambda/3$ neutrons is observed at q = 0.912 and has been deleted from the data. The symmetric splitting about the Cr(0 0 1) position shows that the Cr layers form a transverse SDW with $\boldsymbol{Q}$ normal to the layers. No evidence of a longitudinal SDW is observed. The period of the SDW is in close agreement with bulk Cr, which

attests to the high quality of the Cr layers in the sample. Strain, impurities and defects have a dramatic effect on the SDW period in bulk Cr. Plotted in Fig. 4 are the intensities of the $(1-\delta)$ satellite peaks versus T, which shows the strong thickness dependence of the Cr ordering.

Shown in Fig. 5 is the good agreement between T_N measured by neutron diffraction as compared with transport and magnetization anomalies (as described in the next section). No AF-ordering transition is observed for $t_{Cr} < 42$ Å. For $t_{Cr} < 42$ Å, T_N initially increases quickly and then asymptotically approaches the thick-film value. For a 3000 Å thick Cr film grown in similar fashion to the superlattices, a value of $T_N = 295$ K was obtained.

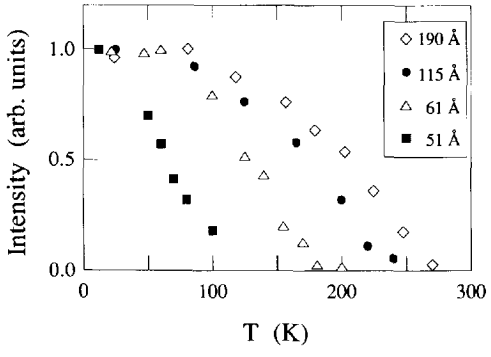

Fig. 4. $(1-\delta)$ satellites peak intensities versus T for [Fe(14 Å)/Cr]$_N$ superlattices of different Cr layer thicknesses.

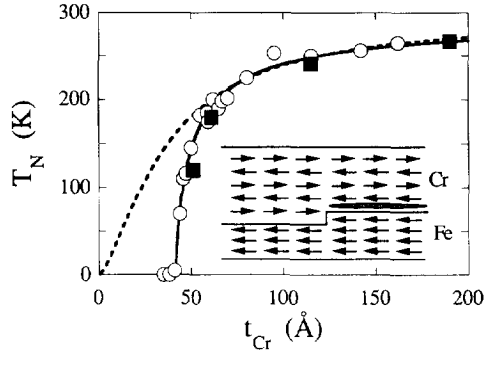

Fig. 5. T_N for a series of [Fe(14 Å)/Cr(t_{Cr})]$_N$ superlattices versus Cr layer thickness. The open circles are the measured resistively and the solid squares are determined from the neutron diffraction results. The dashed line is a fit to Eq. (2). The inset shows a possible spin configuration of Cr on a stepped Fe surface in which the region of spin frustration at the Fe–Cr interface is shown schematically by the shaded ellipse to the right of the atomic step.

4. Interlayer coupling

The AF-ordering of the Cr dramatically alters the coupling of the Fe layers. Shown in Fig. 6 are magnetization M and magnetotransport $(\Delta\rho/\rho)$ measurements above T_N for the sample shown in Fig. 2. The first quadrant of the hysteresis loops in decreasing field is shown with H along the Fe easy and hard axes. As H decreases, the hard-axis magnetization gradually decreases from saturation M_s to its remanent value $M_r \approx 0.7 M_s$ for all temperatures. This behavior is expected for coherent rotation of Fe layers towards the easy axis with an expected M_r of $M_s/\sqrt{2}$. For $T > T_N$, the easy-axis M decreases sharply at low fields to $M_r \approx 0.54 M_s$. This suggests biquadratic coupling of the Fe layers in which alternate moments are aligned parallel and perpendicular to the field consistent with Ref. [23]. The 90° alignment of the Fe layers at low fields gives the expected enhanced magnetoresistance. The shape of both the magnetization and magnetoresistance curves are consistent with a combination of biquadratic coupling and cubic anisotropy. Below T_N, there is a dramatic change in both quantities: there is an increase in M_r along the easy axis and a decrease in the saturation field of the hard axis which both suggest that the biquadratic coupling is suppressed. Shown in Fig. 7 are the saturation $\Delta\rho/\rho$ values and saturation fields H_s versus T. H_s in Fig. 7, is defined as the field at which the sharp drop in the easy-axis magnetization and rise in the magnetoresistance occurs. Both $\Delta\rho/\rho$ and H_s are strongly T dependent and show anomalies at the measured value of T_N.

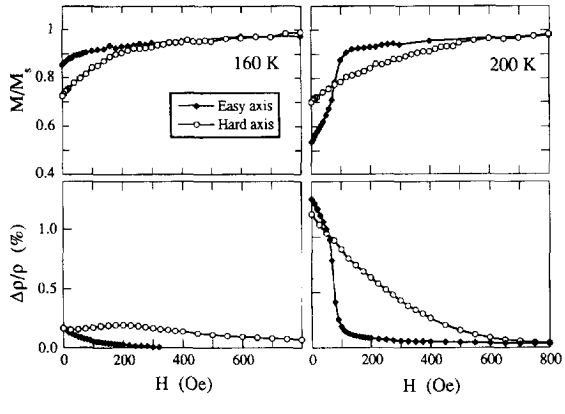

Fig. 6. Upper quadrant of the magnetization and magnetoresistance measured along the easy and hard axes for the same [Fe(14 Å)/Cr(74 Å)]$_{20}$ superlattice as shown in Fig. 2. The left panels are measured at 160 K and the right panels at 200 K. $T_N = 187$ K.

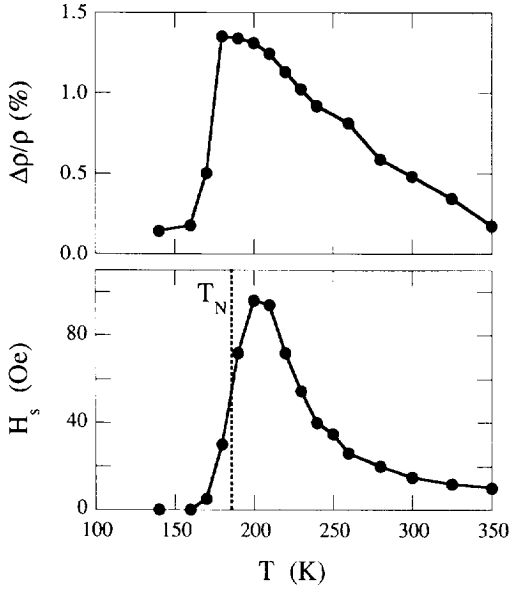

Fig. 7. (a) Saturation magnetoresistance $\Delta\rho/\rho$ and (b) saturation field, H_s versus T for the [Fe(14 Å)/Cr(74 Å)]$_{20}$ superlattice shown in Figs. 2 and 6. The vertical line is T_N.

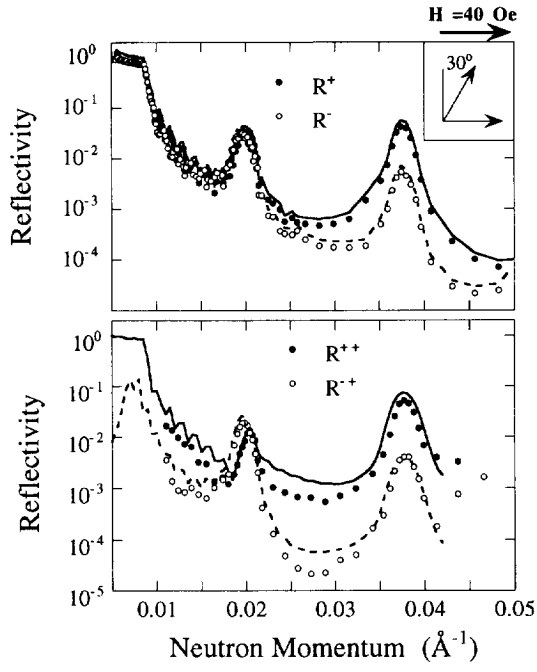

Fig. 8. Neutron reflectivity for [Fe(14 Å)/Cr(74 Å)]$_{20}$ measured with (R^{++} and R^{--}) and without (R^{-} and R^{-}) polarization analysis along the easy axis at $H = 40$ Oe and $T = 205$ K. The lines are the fit to the data for the spin structure shown in the inset.

Polarized neutron reflectivity on the sample shown in Figs. 2 and 6 was used to confirm the 90 configuration of the Fe layer. We focus on the 205 and 160 K results that straddle T_N; measurements also were made at 300 and 20 K, as discussed in Ref. [25]. Measurements were made both with and without polarization analysis of the scattered neutrons. The reflectivity of the sample for the initial polarization of the beam parallel and antiparallel to H is given by R^+ and R^-, respectively. Using an analyzer after the sample we measure the non-spin-flip (NSF) reflectivity, R^{++} and the spin-flip (SF) reflectivity R^{-+}. The relation between these quantities is given by $R^- = R^{+-} + R^{--}$, $R^- = R^{-+} + R^{--}$, and $R^{--} = R^{+-}$. The NSF reflectivities R^{++} and R^{--}, depend upon both the nuclear scattering potential bN and the component of magnetization parallel (or anti-parallel) to the neutron spin. The difference between R^{++} and R^{--} is a measure of the component of the sample magnetization parallel to H. The SF reflectivity contribution arises solely from the perpendicular component of M and is zero if this component is not present.

Shown in Fig. 8 are reflectivity results measured at 205 K with $H = 40$ Oe along the easy axis. The measurements were taken over a range of momenta $k = 2\pi \sin\theta/\lambda$ (where θ is the angle of incidence of the neutrons on the surface and λ is the neutron wavelength) from the region of total reflection up to and including the first superlattice Bragg reflection at $k = 0.037$ Å^{-1}. The spectra consist of two Bragg peaks and higher-frequency Kiessig oscillations resulting from the finite size of the superlattice. The F-peak at high k corresponds to the superlattice periodicity and results from both the nuclear scattering from the layers and components of the Fe-layer magnetization that are ferromagnetically aligned with H. The AF-peak at lower k, present for all four reflectivity curves, corresponds to a doubling of the unit cell and is a signature of interlayer coupling [26]. The presence of this peak in the SF reflectivity indicates that there is a perpendicular component of M with a repeat distance of twice the superlattice spacing. The width of the peak indicates that the magnetic structure is coherent over the entire thickness of the superlattice.

We fitted the reflectivity data in the conventional manner by assigning a refractive index to each layer and matching boundary conditions to calculate the total reflectivity. We assume a two-sublattice model where the angle of magnetization of each sublattice with respect to H are the fitting parameters. The lines shown in Fig. 8 are fits to the data which determine the magnetic structure shown in the inset to Fig. 8. (Note that all magnetizations are in-plane: parallel and perpendicular refer to in-plane directions with respect to the field.) The tilt away from

the 90° arrangement is due to the Zeeman energy, which makes it energetically favorable for M to cant toward H; measurements at 6 Oe show a substantial decrease in the tilt and the system approaches the expected 0 and 90° configuration at $H = 0$. Hard-axis measurements (with polarization analysis) made at the same T and H as for the easy axis measurements show that the AF peak arises solely from spin-flip scattering, as would be expected for a configuration in which the moments of subsequent layers are alternatively aligned at 45°, −45° to H.

The results at 160 K are quite sensitive in the way the sample is cooled and the field history. Data were collected in three different ways: (i) Initially the sample was cooled from 205 K in 40 Oe. This produced a structure in which the AF peak is extremely small, indicating that the sample is almost completely ferromagnetically aligned. (ii) The sample is cooled to 160 K in a low field (6 Oe), and the AF peak is still present with only a slight decrease in intensity. (iii) The sample is initially saturated from 6 Oe to 3.5 kOe at 160 K and then the field is reduced back to 6 Oe, comparable to the conditions under which the magnetization was measured. In agreement with the square hysteresis loop, this showed a complete absence of the AF peak. The F peak did not change in width, intensity or polarization. This result suggests that at 160 K, the layers are truly uncoupled. When the spins are in a 90° alignment, each Fe layer is along a crystallographic easy axis. When cooled below T_N in a low field, the Fe layers remain in this metastable configuration. Applying a modest field aligns the layers and the system cannot get back to the 90° configuration without warming above T_N.

5. Discussion and conclusions

In summary, we have investigated the AF ordering of Cr layers in epitaxial Fe/Cr(0 0 1) superlattices and report the following observations: (i) AF order is suppressed for $t_{Cr} < 42$ Å, (ii) for $t_{Cr} > 42$ Å, T_N initially rises rapidly, and then asymptotically approaches its thick-film value, (iii) the AF order of the Cr layers is characterized by a transverse SDW consistent with that of bulk Cr, and (iv) the strongly T-dependent biquadratic coupling observed for $T > T_N$ is suppressed for $T < T_N$.

A variety of factors can alter T_N values of Cr, including impurities, pressure, defects, grain size and epitaxial strains. However, the close agreement of the SDW wavelength with the bulk value would suggest that the change in T_N is not a result of impurities or strain, which would alter the Fermi surface and, therefore, the SDW wavelength. We argue instead, that the T_N versus t_{Cr} can be understood as arising from a combination of finite-size effects within the Cr spacer and spin-frustration effects at the Fe–Cr interface. Scaling theory predicts that T_N should have the following thickness dependence:

$$\frac{T_N(\infty) - T_N(t_{Cr})}{T_N(t_{Cr})} = b t_{Cr}^{-\lambda}, \tag{2}$$

where $\lambda = 1/\nu$ is the shift exponent, ν is the correlation-length exponent for the bulk system, and b is a constant [27]. The theoretically expected λ values are 1.419 and 1.5884 for the 3D Heisenberg and Ising models. Shown by the dashed line in Fig. 5, is Eq. (2) fitted to the data for $t_{Cr} \geq 70$ Å, where $T_N(\infty) = 295$ K, the thick film limit and $\lambda = 1.4 \pm 0.3$ in close agreement with scaling theory.

For $t_{Cr} < 70$ Å, the measured T_N versus t_{Cr} breaks away from scaling theory and the magnetic ordering is suppressed for $t_{Cr} < 42$ Å. We believe that this behavior arises from spin-frustration effects in the vicinity of rough Fe–Cr interfaces. Such interfaces contain atomic steps as shown in the Fig. 5 inset and the interfacial exchange energy can be minimized only locally. This argument is in the same spirit as Slonczewski's proximity magnetism model for biquadratic coupling which arises from the local ordering of Cr layer in the terrace regions giving rise to local F or AF coupling. However, if the Cr layer orders long-range (i.e. AF-domain size is much larger than the terrace dimensions) then frustration of the interfacial spins will occur. In Fig. 5 inset, excess magnetic energy is schematically located at the Fe–Cr interface to the right of the step where the Fe and Cr moments are forced to align ferromagnetically. The value of T_N, therefore, should be influenced by a balance between the energy gained from long-range AF ordering of the Cr and the energy cost due to magnetic frustration at the Fe–Cr interfaces.

For thin Cr layers, the frustration energy is sufficiently high to suppress long-range ordering of the Cr. Recent theoretical calculation of Cr ordering on Fe layers show that the Cr ordering is sensitive to both interdiffusion [28] and steps [29, 30] at the Fe–Cr interface. The presence of frustrated Fe–Cr bonds can strongly suppress the Cr moment over extended distances. As t_{Cr} increases, the system overcomes the frustration energy and begins to order. Such a crossover (from local to long-range ordering) behavior has been seen in simple mean-field calculations at finite temperatures for an AF-layer sandwiched between two ferromagnetic layers in the presence of steps [31]. The crossover thickness for the present samples is 42 Å of Cr.

For the thicker Cr layers ($t_{Cr} > 65$ Å), the long-period oscillatory coupling energy has decreased to a value of < 0.01 erg/cm^2 and the observed coupling is dominated by a non-oscillatory biquadratic term. The biquadratic coupling decays slowly with Cr thickness and has been observed for thicknesses as large as 160 Å. Both the slow

decay and the suppression of the coupling at T_N can be understood within Slonczewski's fluctuation or proximity magnetism models. Both models suggest that the Cr spins respond locally to fluctuations in the Cr thicknesses giving regions of F or AF coupling. Since the short-period coupling involves the nested region of the Cr Fermi surface, the magnetic interaction should decay more slowly than the long-period coupling. However, below T_N, the neutron diffraction results indicate that the Cr spins order long range with large magnetic domains. If these domains are large compared to the lateral separation of the Cr thickness fluctuations, the Cr layers will no longer respond locally to the thickness fluctuations and the biquadratic coupling with be suppressed. The validity of these models may be further tested by studying the biquadratic coupling strength dependence on crystallographic orientation [8] and interfacial roughness [17].

Acknowledgements

Work supported by the U.S. Department of Energy, Basic Energy Sciences–Materials Sciences, under contract No. W-31-109-ENG-38. Work at ORNL supported by the US Department of Energy, Division of Materials Sciences, under contract No. DE-AC05-84OR21400.

References

[1] P. Grünberg, R. Schreiber, Y. Pang, M.B. Brodsky and C.H. Sowers, Phys. Rev. Lett. 57 (1986) 2442.
[2] S.S.P. Parkin, N. More and K.P. Roche, Phys. Rev. Lett. 64 (1990) 2304.
[3] J. Ungaris, R.J. Celotta and D.T. Pierce, Phys. Rev. Lett. 67 (1991) 140.
[4] S.T. Purcell, W. Folkerts, M.T. Johnson, N.W.E. McGee, K. Jager, J. aan de Stegge, W.B. Zeper, W. Hoving and P. Gruneberg, Phys. Rev. Lett. 67 (1991) 903.
[5] M.N. Baibich, J.M. Broto, A. Fert, F. Nguyen Van Dau, F. Petroff, P. Etienne, B. Greuzet, A. Friederich and J. Chazelas, Phys. Rev. Lett. 61 (1988) 2472.
[6] M. Ruhrig, R. Schaefer, A. Hubert, R. Mosler, J.A. Wolf, S. Demokritov and P. Grünberg, Phys. Stat. Sol (a) 125 (1991) 635.
[7] For a general review see E. Fawcett, Rev. Mod. Phys. 60 (1988) 209.
[8] E.E. Fullerton, M.J. Conover, J.E. Mattson, C.H. Sowers and S.D. Bader, Phys. Rev. B 48 (1993) 15755.
[9] D.T. Pierce, J.A. Stroscio, J. Unguris and R.J. Celotta, Phys. Rev. B 49 (1994) 14564.
[10] P. Bruno and C. Chappert, Phys. Rev. Lett. 67 (1991) 1602.
[11] J. Mathon, J. Magn. Magn. Mater. 100 (1991) 527.
[12] C.J. Gutierrez, J.J. Krebs, M.E. Filipkowski and G.A. Prinz, J. Magn. Magn. Mater. 116 (1992) L305.
[13] Z. Celinski, B. Heinrich and J.F. Cochran, J. Magn. Magn. Mater. 145 (1995) L1.
[14] J. Ungaris, R.J. Celotta and D.T. Pierce, J. Magn. Magn. Mater. 127 (1993) 205.
[15] U. Rucker, S. Demokritov, E. Tsymbal, P. Grünberg and W. Zinn, J. Appl. Phys., in press.
[16] B. Rodmacq, K. Dumesnil, P. Mangin and M. Hennion, Phys. Rev. B 48 (1993) 3556.
[17] A. Schreyer, J.F. Ankner, M. Schäfer, H. Zabel, C.F. Majkrzak and P. Grünberg, Physica B 198 (1994) 173, Physica B 221 (1996) 366.
[18] For a general discussion see K.B. Hathaway, in: Ultrathin Magnetic Structures II, eds. B. Heinrich and J.A.C. Bland (Springer, Berlin, 1994) p. 45.
[19] S. Demokritov, E. Tsymbal, P. Grünberg, W. Zinn and I.K. Schuller, Phys. Rev. B 49 (1994) 720.
[20] J.C. Slonczewski, Phy. Rev. Lett. 67 (1991) 3172.
[21] J.C. Slonczewski, J. Appl. Phys. 73 (1993) 5957.
[22] J.C. Slonczewski, J. Magn. Magn. Mater. 150 (1995) 13.
[23] E.E. Fullerton, K.T. Riggs, C.H. Sowers, S.D. Bader and A. Berger, Phys. Rev. Lett. 75 (1995) 330.
[24] E. Fawcett, H.L. Alberts, V. Yu. Galkin, D.R. Noakes and J.V. Yakmi, Rev. Mod. Phys. 66 (1994) 25.
[25] S. Adenwalla, G. Felcher, E.E. Fullerton and S.D. Bader, Phys. Rev. B 53 (1996) 2474.
[26] S.S.P. Parkin, A. Mansour and G.P. Felcher, Appl. Phys. Lett. 58 (1991) 1473.
[27] K. Binder, in: Phase Transitions and Critical Phenomena, eds. C. Domb and J.L. Lebowitz (Academic Press, London, 1983) p. 1.
[28] D. Stoeffler and F. Gautier, Phys. Rev. B 44 (1991) 10389.
[29] D. Stoeffler and F. Gautier, J. Magn. Magn. Mater. 147 (1995) 260.
[30] A. Vega, C.Demangeat, H. Dreyssé and A. Chouairi, Phys. Rev. B 51 (1995) 11546.
[31] E.E. Fullerton, K.T. Riggs, C.H. Sowers, S.D. Bader and A. Berger, MRS Symposia Proc., 1995 Spring Meeting of the Material Research Society, San Francisco, CA, 17–21 April 1995, Mat. Res. Soc. Symp. Proc. 384 (1995) 145.